JOURNAL OF AIRCRAFT
Vol. 36, No. 2, March–April 1999

Selection of Sensor Locations for Active Vibration Control of Helicopter Fuselages

C. Venkatesan* and A. Udayasankar†
Indian Institute of Technology, Kanpur 208 016, India

Vibration control has always been a challenging problem to the helicopter designer. This paper addresses the problem of the formulation and solution of an active vibration control scheme for helicopters, based on the concept of active control of structural response. First, using a mathematical procedure employing the Fisher information matrix, optimum sensor locations have been identified in a three-dimensional model of a flexible fuselage structure. The reference parameters used in the selection process are the elements of a vector defined as the effective independence distribution vector and the condition number of the Fisher information matrix. It is observed that, irrespective of the excitation frequency, these optimally selected sensor locations experience relatively high levels of vibration. Then, using the measurement from these optimal sensor locations, a multi-input/multi-output control problem has been formulated and solved to obtain the active control forces required for vibration minimization in the helicopter fuselage. It is observed that sensor locations have a significant influence on the level of vibration reduction in a fuselage structure.

Nomenclature

$[A]$, $[B]$, $[C]$ = system, control, and output matrices, respectively
C_i, C^i = damping of the ith gearbox mounting
$[C]_s$ = output matrix defined for preselected sensor locations
E = idempotent matrix
$\{F\}$, $\{f\}$ = forcing function vector
$\{F_{Hx}, F_{Hy}, F_{Hz}\}$ = hub shears in the nonrotating hub-fixed coordinate system
F^i = force at the ith gearbox mounting
F_s^i, F_D^i, F_c^i = spring, damper, and control force at ith gearbox mounting
$\{I_{xx}, I_{yy}, I_{zz}\}_F$ = mass moment of inertia of fuselage
$\{I_{xx}, I_{yy}, I_{zz}\}_{GB}$ = mass moment of inertia of gearbox
K_i, K^i = stiffness of the ith gearbox mounting
M_A = number of available sensors
$[\bar{M}]$, $[\bar{C}]$, $[\bar{K}]$ = modal mass, damping, and stiffness matrices, respectively
$[M]_F$, $[C]_F$, $[K]_F$ = mass, damping, and stiffness matrices of fuselage in finite element domain
$\{M_{Hx}, M_{Hy}, M_{Hz}\}$ = hub moments in the hub-fixed nonrotating coordinate system
M_L = initial number of candidate sensor locations
m_B = rotor blade mass
m_F = mass of fuselage
m_{GB} = mass of gearbox
NB = number of blades in the rotor system
Nm = number of flexible modes of the fuselage
$\{Q\}_F$ = generalized force vector
$\{q\}$ = state vector consisting of degrees of freedom of gearbox and fuselage modes
R = rotor radius
$\{R_{Hx}, R_{Hy}, R_{Hz}\}$ = perturbational translation of the hub
$\{U\}$ = control force vector
$\{x\}$ = vector of nodal degrees of freedom
$\{Y_s\}$ = vibratory response at preselected sensor locations
$\{y\}$, $\{Y\}$ = output vector
β_F = structural damping coefficient
$\{\eta\}$ = modal coordinate vector
$\{\hat{\eta}\}$ = estimate of the states of the system
$\{\Theta_{Hx}, \Theta_{Hy}, \Theta_{Hz}\}$ = angular displacement of the hub
$\{\Phi\}$ = modal matrix
$\{\Phi_s]$ = modal matrix corresponding to initial set of candidate sensor locations
Ω = rotor angular velocity
$\{\ \}_F$, $[\ ]_F$ = quantities corresponding to fuselage
$\{\ \}_{GB}$, $[\ ]_{GB}$ = quantities corresponding to gearbox

Received Dec. 31, 1997; revision received Aug. 31, 1998; accepted for publication Sept. 15, 1998.

*Associate Professor, Department of Aerospace Engineering. Senior Member AIAA.

†Graduate Student, Department of Aerospace Engineering; currently Assistant Systems Engineer, CAD/CAM Group, TCS India Limited, Chennai, India.

I. Introduction

THE periodic loads of rotor systems cause vibration in helicopters. With increasing demand for high-speed and high-performance helicopters, vibration control has become an important objective in the design of modern helicopters. References 1–3 provide excellent reviews of helicopter vibration and its control. Over the years, the vibratory levels in the fuselage of helicopters have been reduced by using passive vibration control devices and/or by suitable structural design. For present-day helicopters, the general requirement is to have a maximum vibratory level of $0.1g$ in the fuselage. However, in the future, with the adoption of stringent vibration control, it will become necessary to reduce the vibratory levels below $0.05g$, or even $0.02g$.[4]

Vibration reduction schemes adopted in helicopters can be classified as either passive or active control methodologies. The passive control scheme includes hub or blade-mounted pendulum absorbers; antiresonant vibration isolation devices like dynamic antiresonant vibration isolator (DAVI), antiresonant isolation system (ARIS), and liquid inertia vibration eliminator (LIVE); structural modifications; and structural optimization. Active control methodologies include higher harmonic control (HHC), individual blade control (IBC), active flap control (AFC), and active control of structural response (ACSR). It may be noted that while HHC, IBC, and AFC control schemes are aimed at reducing the blade loads in the rotating

frame, ACSR is employed in the nonrotating frame to nullify the effect of vibratory hub loads on the fuselage.

The concept of an ACSR scheme is based on the principle of superposition of two independent responses of a linear system, such that the total response is zero. In the case of helicopters, the fuselage is excited by the application of controlled external actuators at selected locations, such that the total response of the fuselage caused by the rotor loads and the external actuator forces is a minimum.[5-10] A schematic of the helicopter system with the ACSR scheme is shown in Fig. 1. The rotor loads (F_{Hx}, F_{Hy}, F_{Hz}, M_{Hx}, M_{Hy}, and M_{Hz}) are transmitted to the fuselage through the gearbox support structure. The support structure is idealized as a spring, damper mechanism, and a control force generator. In a passive scheme, the control force generator corresponds to a vibration absorber mass (as in ARIS), whereas in the case of ACSR, the control force generator is an active electrohydraulic force actuator. Preliminary studies based on extensive ground and flight tests have shown promising results in reducing the vibration in helicopters. The major advantages of the ACSR scheme are 1) less power requirements, 2) minimal airworthiness requirements because this scheme is independent of the primary flight-control systems, and 3) selectively minimized vibratory levels at any set of chosen locations in the fuselage.

A key aspect of vibration control is the measurement of vibration. In general, the vibratory levels are measured at tail boom/tail rotor transmission, cockpit instrument mountings, cabin floor, and pilot location.[8-10] Even though these locations may be sensitive, in the light of recent developments[11-13] on the optimal placement of sensors for system identification, an interesting question arises: i.e., whether or not the measurement of vibration at the previously mentioned locations truly represents the vibratory levels in the structure. In other words, whether or not the control of vibration at some selected sensitive points in the structure truly corresponds to a reduction of vibration in the whole structure. A review on the sensor placement in distributed parameter (continuous) systems can be found in Ref. 14. It is pointed out in Ref. 13 that the measurement locations play a major role in the quality of measurement, and in some situations, modes may be completely missed. For a simple one-dimensional structure, the measurement locations can be selected based on experience, but for complicated three-dimensional structures, the choice is very difficult. Therefore, there is need for a systematic approach based on mathematical principles to arrive at the optimal sensor locations. Kammer[11] described a suboptimal procedure for identifying the sensor locations in large structures for the measurement of frequencies and mode shapes, which can be compared with finite element method results for correlation studies. This procedure is based on using the Fisher information matrix and effective independence distribution vector (EIDV) to eliminate sequentially the redundant sensor locations from an initial set of many candidate sensor locations. In Ref. 12, this approach was slightly modified by using the controllability and observability matrices of the system to identify the actuator/sensor placement in a truss structure for modal parameter (natural frequency and mode shape) identification. A comparative analysis of the EIDV method and the Guyan reduction approach is presented in Ref. 13. The comparative study was based on identifying the sensor locations for modal testing of one-dimensional beams and two-dimensional plates. The EIDV method of identifying the sensor locations in a systematic manner is computationally elegant and has been shown to be successful.[13] However, the demonstrative applications have been to rather simple structures and have emphasized measurements for vibration testing.

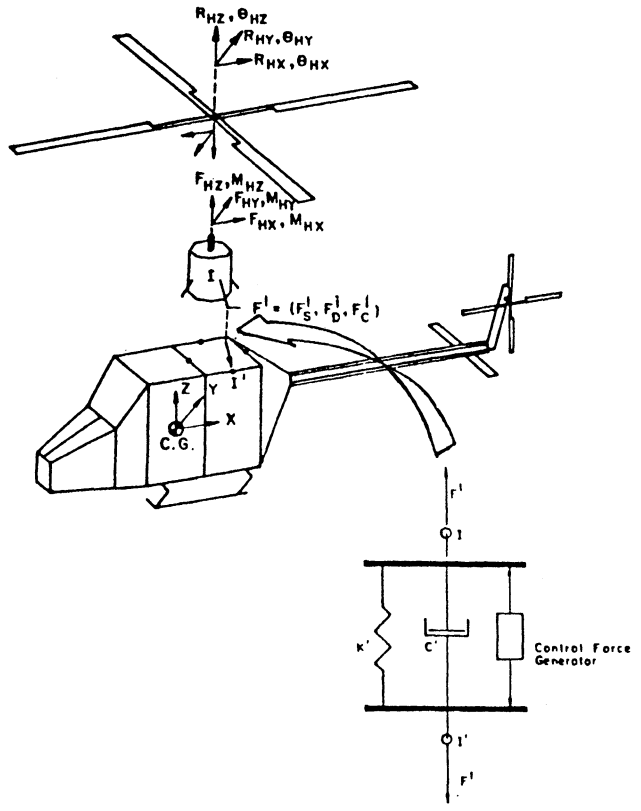

Fig. 1 Interaction of subsystems in helicopters.

An interesting feature of helicopter fuselage structure is that the airframe has only a small distributed structural mass in comparison with several large concentrated masses, representing engine, gearbox, rotor systems, etc. Therefore, the helicopter fuselage structure has a high modal density, i.e., many closely spaced natural frequencies, and very complex mode shapes.[15] Considering the mathematical simplicity of the EIDV approach and the complexity of the helicopter fuselage vibrations, the application of the EIDV approach for active control of vibrations in helicopters will be highly useful from the point of view of practical considerations.

The main objectives of the present study are as follows:

1) Identification of optimal sensor locations for measurement of vibration in a three-dimensional finite element model of a helicopter fuselage for active control studies.

2) Analysis of vibratory levels observed at the optimally selected sensor locations.

3) Formulation of an open-loop control scheme for vibration minimization using the ACSR scheme.

4) Analysis of the effectiveness of vibration control using the measurements from optimally placed sensors, in comparison with the control of vibration using measurements from arbitrarily placed sensor locations.

In this paper, the terminology, optimal sensor locations, essentially implies a suboptimal set of sensor locations, because the EIDV approach is a suboptimal method.

II. Mathematical Formulation

The mathematical formulation consists of three parts. They are 1) description of the method for the selection of sensor locations for vibration measurement, 2) equations of motion of the rotor–gearbox–fuselage system, and 3) formulation of the control scheme. A brief description of these three items is provided next. The details of the derivation can be found in Ref. 16.

A. Mathematical Scheme for the Selection of Sensor Locations

The equations of motion of a flexible structure in a finite element domain can be written as

$$[M]_F\{\ddot{x}\} + [C]_F\{\dot{x}\} + [K]_F\{x\} = \{F\} \tag{1}$$

Considering the first Nm undamped modes, the modal transformation relation can be written as

$$\{x\} = [\Phi]\{\eta\} \tag{2}$$

Substituting Eq. (2) in Eq. (1), and premultiplying by $[\Phi]^T$, the equations of motion in modal space can be written as

$$[\bar{M}]\{\ddot{\eta}\} + [\bar{C}]\{\dot{\eta}\} + [\bar{K}]\{\eta\} = \{Q\}_F \tag{3}$$

where $[\bar{M}]$, $[\bar{C}]$, $[\bar{K}]$ have a dimension of $Nm \times Nm$, and $\{\eta\}$, $\{Q\}_F$ are vectors of size $Nm \times 1$.

Assuming harmonic input excitation $\{F\} = \{\bar{F}\}e^{i\omega t}$, where ω is a constant. The steady-state displacement at any point on the structure can be expressed as

$$\{y\} = [\Phi_s]\{\eta\} \tag{4}$$

where the dimension of $\{y\}$ is $M_L \times 1$, and M_L represents the initial number of candidate sensor locations. Φ_s represents the modal matrix corresponding to the initial set of candidate sensor locations.

It is assumed that the initial number of candidate sensor locations is greater than the number of modal coordinates, i.e., $M_L > Nm$. In state feedback control, an estimate of the states of the system is required, and the best estimate can be obtained from the following equation (for the sake of simplicity, it is assumed that there is no measurement noise):

$$\{\hat{\eta}\} = \underbrace{[\Phi_s^T\Phi_s]^{-1}\Phi_s^T}\{y\} \tag{5}$$

The underbraced term in Eq. (5) is denoted as the generalized inverse (also known as Moore–Penrose inverse or pseudoinverse) of Φ_s.[17] Because the dimension of Φ_s is $(M_L \times Nm)$ and $M_L > Nm$, the rank of Φ_s is equal to Nm, which is the same as the number of modal coordinates. Hence, there are $(M_L - Nm)$ rows in Φ_s, which are linearly dependent on the remaining Nm rows. Physically, it means that there are $(M_L - Nm)$ additional sensors, providing redundant information about the Nm modal coordinates. From the point of view of reachability of certain locations and also as a result of the cost of sensors, it is not possible to have sensors at all locations. Generally, the number of available sensors (M_A) is less than the number of initial candidate measurement locations, and it can be greater than or equal to the number of modes, i.e., $Nm \leq M_A < M_L$. The aim is to eliminate those sensors that provide redundant information about the system response. In Eq. (5), the symmetric matrix $[\Phi_s^T\Phi_s]$ is denoted as the Fisher information matrix. Premultiplying Eq. (5) by Φ_s yields

$$\Phi_s\{\hat{\eta}\} = \underbrace{\Phi_s[\Phi_s^T\Phi_s]^{-1}\Phi_s^T}\{y\} = \{\hat{y}\} \tag{6}$$

In Eq. (6), $\{\hat{y}\}$ can be identified as the reconstructed output using the estimate of the states $\{\hat{\eta}\}$. If Φ_s is a nonsingular square matrix, then the underbraced term in Eq. (6) will be a unit matrix. For a general case, let the underbraced term in Eq. (6) be denoted by the symbol E:

$$E = \Phi_s[\Phi_s^T\Phi_s]^{-1}\Phi_s^T \tag{7}$$

Matrix E is an idempotent matrix, i.e., $E = E^2$, and its eigenvalues are either 0 or 1. In addition, the trace of the idempotent matrix E is equal to its rank.[17] Hence, the diagonal elements of E represent the fractional contribution to the rank of E and the smallest diagonal element i.e., E_{ii}, contributes the least to the rank of E. Because the rank of E is equal to the rank of Φ_s, the ith row of Φ_s contributes the least to the rank of Φ_s. Therefore, the ith row of Φ_s can be eliminated without influencing its rank. After eliminating the ith row, the modified Φ_s having a reduced size is used to compute the new E matrix, and the process of elimination is repeated. This procedure is carried out sequentially until the number of rows of Φ_s is equal to the number of available sensors M_A. Because this procedure employs a sequential elimination process, it is a suboptimal method. The vector formed by the diagonal elements of E is denoted as the EIDV.

Because the inverse of Fisher information matrix is required to estimate the modal vector, [Eq. (5)], it is important to monitor its condition number at every iteration. If there is a drastic increase in the condition number, then the elimination process must be terminated. The condition number of a square matrix represents the sensitivity of its inverse to very small changes in the elements of the matrix.[18]

In every iteration, one can eliminate either one row (one sensor) or a group of rows (group of sensors), whose corresponding diagonal elements (E_{ii}) are very small in comparison with the other diagonal elements. In identifying the optimal sensor locations, the advantage of group elimination is that it requires less iterations than a series of single eliminations. However, the disadvantage will be that there is a likelihood of increasing the condition number of the Fisher information matrix. This important conclusion has been brought out in Ref. 19 while addressing the problem of the effectiveness of the selection procedure for optimal sensor locations, i.e., single elimination vs. group elimination. In addition, Ref. 19 also addresses the sensitivity of sensor locations to structural modifications.

It is important to note that the selection of optimal sensor locations is not influenced by the type of normalization performed on the modal vectors. However, the condition number of the Fisher information matrix is dependent on the type of normalization, and it can be varied arbitrarily by using different multiplication factors for different modal vectors.[16] Because the condition number is primarily monitored for terminating the elimination process, the variation in the order of the condition number is more important than the absolute value itself.

B. Equations of Motion

For the purpose of application of optimal sensor locations to vibration reduction problems, the coupled rotor–gearbox–fuselage dynamic model was simplified. The simplified model, shown in Fig. 2, consists of a gearbox supported on the top of the fuselage at four locations. The rotor blade dynamics are not included. However, the vibratory hub loads are assumed to be acting at the top of the gearbox, simulating a ground test condition. The gearbox support is idealized as a spring, a viscous damper, and an active control force generator for the

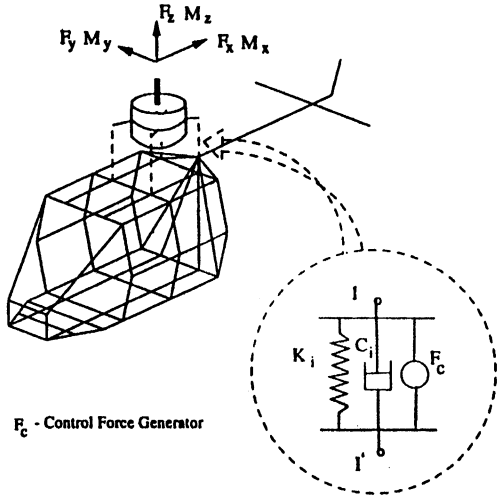

Fig. 2 Coupled gearbox–fuselage dynamic model.

vibration minimization. For the sake of simplifying the analysis and also because of the unavailability of practical data, several assumptions have been made in formulating the equations.

1. Assumptions

1) The gearbox is assumed to be rigid and undergoes only vertical translation, pitch, and roll motions.

2) The fuselage is assumed to be undergoing rigid-body vertical translation, pitch, and roll motions, as well as flexible deformation as a result of elastic modes.

3) The gearbox supports are assumed to be uniaxial members, providing forces only in the z direction.

4) The c.m. of the gearbox is assumed to be above the c.m. of the fuselage and on the same vertical axis.

5) The rigid-body rotational motions of the gearbox and fuselage are assumed to be small. Hence, the nonlinear terms involving products of rigid-body rotational degrees of freedom have been neglected.

6) The products of inertia of the gearbox and fuselage are assumed to be zero.

2. Equations of Motion of Coupled Gearbox–Fuselage System

The equations of motion of the coupled gearbox–fuselage system can be written in three sets. Set I describes the rigid-body equations of motion of the gearbox, set II presents the rigid-body equations of motion of the fuselage, and set III represents the equations of motion of the elastic modes of the fuselage. The details of the equations are given in Ref. 16.

C. Vibration Control

During forward flight, the predominant frequency of the periodic hub loads is *NB*/rev. These vibratory loads excite the fuselage structure. The vibratory levels in the fuselage are measured by a set of sensors placed at selected locations. Using the measurement from the sensors, an open-loop multi-input/multi-output (MIMO) control scheme is formulated to minimize the vibration in the fuselage.

The equations of motion of the gearbox–fuselage model are coupled ordinary differential equations, having a harmonic input representing *NB*/rev hub loads. These equations can be written in state-space form as

$$\{\dot{q}\} = [A]\{q\} + B\{U\} + \{f\} \tag{8}$$

The details of system matrices $[A]$ and $[B]$ are given in Ref. 16. The output vector representing the response of the structure can be represented by

$$\{Y\} = [C]\{q\} \tag{9}$$

For harmonic input $\{f\} = \{\bar{f}\}r^{i\omega t}$, the steady-state response can be written as

$$\{q\} = [A - i\omega I]^{-1}[B]\{U\} + [A - i\omega I]^{-1}\{f\} \tag{10}$$

Using Eq. (9), the vibratory response measured at preselected sensor locations can be written as

$$\begin{aligned}\{Y_s\} &= [C]_s\{q\} \\ &= [C]_s[A - i\omega I]^{-1}[B\{U\} + \{f\}] \\ &= [T]\{U\} + \{b\}\end{aligned} \tag{11}$$

where

$$[T] = [C]_s[A - i\omega I]^{-1}[B]$$

$$\{b\} = [C]_s[A - i\omega I]^{-1}\{f\}$$

Formulating a minimization problem as

$$\min \quad J = \{Y\}_s^T\{Y\}_s \quad \text{w.r.t.} \quad \{U\} \tag{12}$$

the best estimate of the control vector minimizing the performance index J can be written as

$$\hat{U} = -[T^TT]^{-1}T^Tb \tag{13}$$

Substituting $\{\hat{U}\}$ from Eq. (13) into Eq. (10), and using Eq. (9), the controlled vibratory response at any location in the coupled gearbox–fuselage system can be obtained. It is important to note that the control force vector $\{\hat{U}\}$ is estimated using the vibratory response at only certain preselected locations in the system. For example, these preselected locations could be the optimally identified locations or they could represent any set of arbitrary locations.

III. Results and Discussion

Using the dynamic model of the coupled gearbox–flexible fuselage system, several studies were performed. The results of these studies are presented in three sections. Section III.B describes the results pertaining to the choice of sensor locations for vibration measurement. A study on the validity of these optimal sensor locations is presented in Sec. III.C. The results on vibration control are presented in Sec. III.D.

Before presenting the results corresponding to the helicopter fuselage model, an example problem has been solved to highlight the essential features of the EIDV approach.

A. Example Problem

Consider an example in which there are six candidate measurement locations (y_i, $i = 1, \ldots, 6$) and three modes represented by the generalized coordinates (η_1, η_2, and η_3), which is given as

$$\begin{Bmatrix} y_1 \\ y_2 \\ y_3 \\ y_4 \\ y_5 \\ y_6 \end{Bmatrix} = \begin{bmatrix} 1 & 0 & 0 \\ 0 & 1 & 0 \\ 0 & 0 & 1 \\ 2 & 0 & 0 \\ 3 & 0 & 0 \\ 4 & 2 & 0 \end{bmatrix} \begin{Bmatrix} \eta_1 \\ \eta_2 \\ \eta_3 \end{Bmatrix} \tag{14}$$

The three column vectors of Φ_s correspond to the modal displacements at the six measurement locations. In this example, the rank of Φ_s is 3. The fourth and fifth rows of Φ_s are integer multiples of the first row. The sixth row is a linear combination of rows 1 and 2. A sensor placed at location 6 will measure a maximum displacement in modes 1 and 2. A sensor at location 3 is essential to measure the third mode. In this case, a minimum of three sensors are required to estimate the three generalized coordinates. It is essential to have one sensor at location 3, preferable to have the second sensor at location 6, and the third sensor can be placed at any one of the remaining four locations (1, 2, 4, or 5). Using the EIDV approach, the redundant sensor locations are eliminated sequentially one at a time. The results of the sequential elimination are provided in Table 1.

Table 1 contains $[\Phi_s]_j$ and $[E]_j$ (subscript j refers to jth iteration) at every iteration along with the lowest diagonal value of $[E]_j$. In the first iteration, the lowest diagonal value of E is E_{11}, which is 5/86. Therefore, the first row has the least influence on the rank of Φ_s. Eliminating the first row, i.e., the sensor at location 1, the new $[\Phi_s]_2$ is formed for the second iteration. In the second iteration, the lowest diagonal value of $[E]_2$ is E_{33}, which is 20/81. Eliminating this row (note that this row corresponds to sensor location 4 in the original set of six sensor locations), the new $[\Phi_s]_3$ for the third iteration is formed. In the third iteration, the lowest diagonal value of

Table 1 Example problem

Iteration j	$[\Phi_s]_j$	$[E]_j$	Lowest E_{ii}	Condition number
1	$\begin{bmatrix} 1 & 0 & 0 \\ 0 & 1 & 0 \\ 0 & 0 & 1 \\ 2 & 0 & 0 \\ 3 & 0 & 0 \\ 4 & 2 & 0 \end{bmatrix}$	$1/86 \begin{bmatrix} 5 & -8 & 0 & 10 & 15 & 4 \\ -8 & 30 & 0 & -16 & -24 & 28 \\ 0 & 0 & 86 & 0 & 0 & 0 \\ 10 & -16 & 0 & 20 & 30 & 8 \\ 15 & -24 & 0 & 30 & 45 & 12 \\ 4 & 28 & 0 & 8 & 12 & 72 \end{bmatrix}$	5/86	38
2	$\begin{bmatrix} 0 & 1 & 0 \\ 0 & 0 & 1 \\ 2 & 0 & 0 \\ 3 & 0 & 0 \\ 4 & 2 & 0 \end{bmatrix}$	$1/81 \begin{bmatrix} 29 & 0 & -16 & -24 & 26 \\ 0 & 81 & 0 & 0 & 0 \\ -16 & 0 & 20 & 30 & 8 \\ -24 & 0 & 30 & 45 & 12 \\ 26 & 0 & 8 & 12 & 68 \end{bmatrix}$	20/81	37
3	$\begin{bmatrix} 0 & 1 & 0 \\ 0 & 0 & 1 \\ 3 & 0 & 0 \\ 4 & 2 & 0 \end{bmatrix}$	$1/61 \begin{bmatrix} 25 & 0 & -24 & 18 \\ 0 & 61 & 0 & 0 \\ -24 & 0 & 45 & 12 \\ 18 & 0 & 12 & 52 \end{bmatrix}$	25/61	33
4	$\begin{bmatrix} 0 & 0 & 1 \\ 3 & 0 & 0 \\ 4 & 2 & 0 \end{bmatrix}$	$\begin{bmatrix} 1 & 0 & 0 \\ 0 & 1 & 0 \\ 0 & 0 & 1 \end{bmatrix}$	——	33

$[E]_3$ is E_{11}, which is 25/61. Eliminating this row, i.e., the sensor at location 2 in the original set of six locations, the final $[\Phi_s]_4$ is formed. In this case, $[E]_4$ is an identity matrix, indicating that all diagonal elements, i.e., all sensors, are equally important. Further elimination of any one row will render the Fisher information matrix a singular matrix. This means that we are attempting to estimate three generalized (independent) coordinates with two sensor measurements, which is not possible. In this example, the condition number of the Fisher information matrix exhibits a very small variation with iteration.

B. Choice of Sensor Locations for Vibration Measurement

Figure 3 shows a finite element model of a helicopter fuselage. The length of the helicopter model is 8.25 m, the height is 2 m, and the width is 3 m. The fuselage is 4 m long, having a width of 2.5 m and a height of 1.5 m. The tail boom is 4.25 m in length, with a horizontal stabilizer having a span of 3 m attached near the end. In addition, lumped masses representing two engines, a tail gearbox, and two end plates are also attached to the structure at appropriate nodes. The total number of nodes and the degrees of freedom of the finite element model are 64 and 384, respectively. The details of the structural properties, node locations, and other data are given in Ref. 20. It was shown in Ref. 20 that the undamped natural frequencies and mode shapes of this model are similar to those of a realistic helicopter. The first four mode shapes of the fuselage structure are shown in Fig. 4.

Assuming that the main rotor system consists of four blades, the vibratory hub loads will have a nondimensional excitation frequency of 4/rev. For the fuselage model, the nondimensional natural frequency of the 20th flexible mode is 6.41 (Ref. 20), which is 50% more than the excitation frequency (4/rev) of the hub loads. Therefore, the first 20 modes of the helicopter fuselage are considered in the vibration analysis.

Considering three rigid-body modes (heave, pitch, and roll), and the first 20 modes of the fuselage (Nm = 20), the modal matrix Φ_s is formulated. Because the vibratory level in the vertical (z) direction is more predominant, without loss of generality, it is assumed that the sensors measure only the z component of the fuselage vibration. Therefore, in the formulation of Φ_s, the modal displacement in the z direction only is considered. Initially, it is assumed that all 64 nodes are the candidate sensor locations, i.e., M_L = 64. Employing the procedure described in Sec. II.A, the redundant sensor locations were eliminated at each iteration. The final set of 23 optimal sensor locations is indicated by node numbers in Fig. 5.

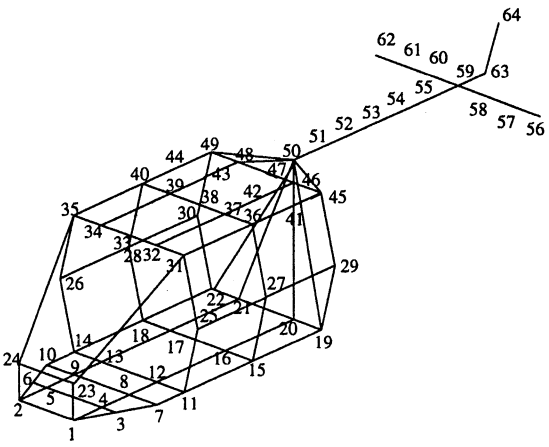

Fig. 3 Finite element model of helicopter fuselage.

C. Validation of Optimal Sensor Locations

A vibration analysis was performed using the coupled gearbox–fuselage equations by applying a vibratory force at the top of the gearbox. The total number of degrees of freedom considered in this analysis is 26. These include three rigid-body modes of the gearbox (heave, pitch, and roll) three rigid-body modes, and 20 flexible modes of the fuselage. The gearbox is assumed to be supported on the roof of the fuselage at the four nodes (39, 48, 46, and 37). The data used for the vibrational analysis are given next.

1) Reference quantities for nondimensionalization: m_B = 65 kg, R = 6 m, and Ω = 32 rad/s.

2) Nondimensional quantities:

K_i = 60.01, C_i = 0.033, m_F = 33.846, m_{GB} = 4.615, I_{xxF} = 0.6838, I_{yyF} = 2.7350, I_{xxGB} = I_{yyGB} = 0.0171, and $F_z/m_B\Omega^2R$ = 0.0001.

Coordinates of fuselage c.g. from origin at the nose of the fuselage: x = 0.5632, y = 0.0, and z = 0.0833.

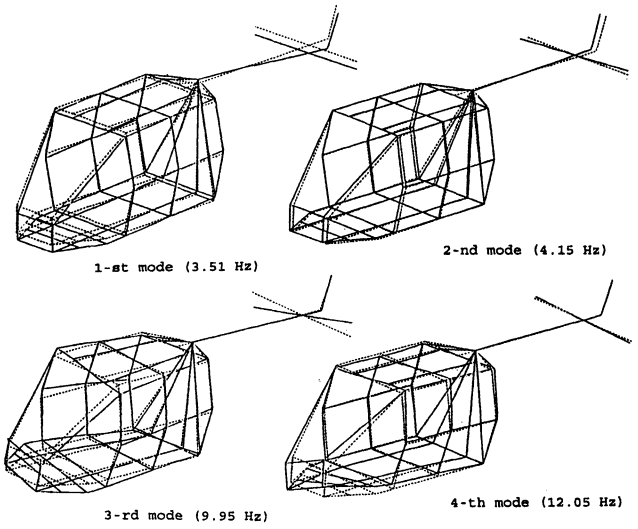

Fig. 4 First four elastic modes of the fuselage. ---, undeformed configuration; ——, deformed shape.

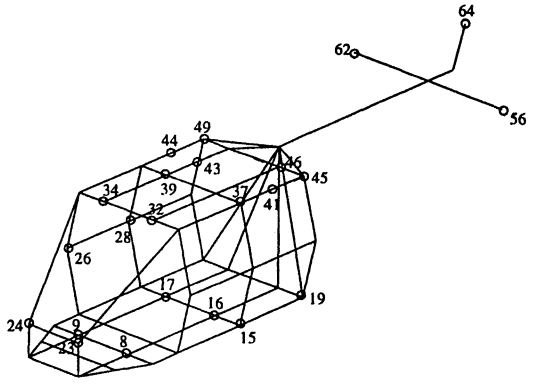

Fig. 5 Optimal sensor locations (sensor locations indicated by node numbers).

Coordinates of gearbox c.g. from origin at the nose of the fuselage: $x = 0.5632$, $y = 0.0$, and $z = 0.3333$.

Structural damping for fuselage elastic modes: $\beta_F = 0.005$.

The vibratory levels in the fuselage were calculated for different excitation frequencies, namely, 1/rev, 2/rev, 3/rev, 4/rev, and 5/rev. For the sake of conciseness, only those results pertaining to the 1/rev and 4/rev excitation frequencies are presented (Figs. 6 and 7). In these figures, the vibratory levels (g levels) at different nodes are indicated by impulses. The arrows (other than the one indicating the gearbox c.g.) indicate the optimal locations for the sensors. For 1/rev excitation, the sensor at node 64 measures the highest level of vibration of 0.48g (Fig. 6). For 4/rev excitation (Fig. 7), the peak response occurs at node 33. There are two sensors at node locations 32 and 34, measuring the second highest level of response. A similar behavior was also observed for other excitation frequencies.[16] These results indicate that, irrespective of the excitation frequency, the optimally selected sensors measure high levels of vibration.

D. Open-Loop Vibration Control

Incorporating the open-loop control scheme described in Sec. II.C, an attempt was made to minimize the vibratory response of the fuselage. The control forces required for vibration minimization were evaluated using measurements from several sets of sensor locations. These different sets of sensor locations correspond to 1) 23 optimally placed sensors; 2) 5 arbitrarily placed sensors (node locations 12, 13, 20, 21, and 64); 3) 10 arbitrarily placed sensors (node locations 1, 2, 20, 21, 31, 35, 50, 56, 62, and 64); and 4) 23 arbitrarily (or a nonoptimal set) placed sensors (node locations 1–22 and 64 representing the fuselage floor and tail, respectively). The nondimensional frequency of the excitation force is assumed to be 4/rev (a four-bladed rotor system is considered). The relevant data are listed in Sec. III.C.

Using the vibratory levels measured at the 23 optimally selected locations, the control forces required for minimization of vibration in the fuselage were calculated. Figure 8 shows a comparison of the baseline vibratory levels along with the controlled response. The fuselage vibratory level has been reduced substantially from the baseline peak acceleration of 0.284g to a level of 0.5E-04g at node location 33. In addition, the vibratory levels at all nodes in the fuselage are reduced to very low levels. The gearbox c.g. experiences an increase in the g level, i.e., the gearbox g level increased from a value of 0.0477g to 0.0625g. This observation of increasing gearbox vibration while reducing fuselage vibrations is similar to the phenomenon observed in an ARIS type of passive vibration control scheme.[21] Figures 9a and 9b show the magnitudes and

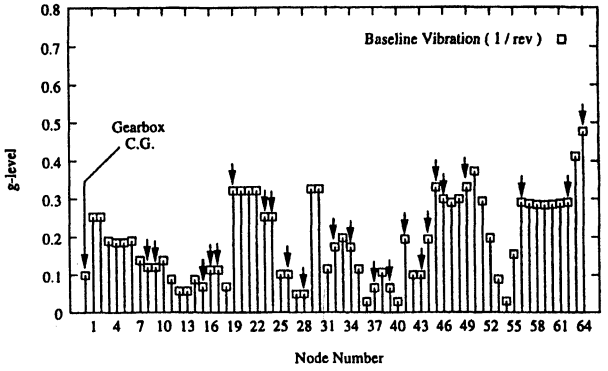

Fig. 6 Baseline vibratory levels (excitation frequency 1/rev).

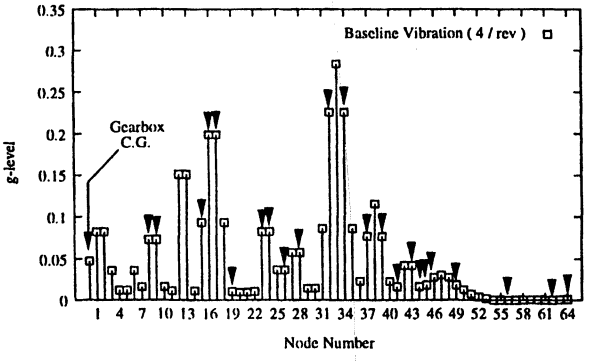

Fig. 7 Baseline vibratory levels (excitation frequency 4/rev).

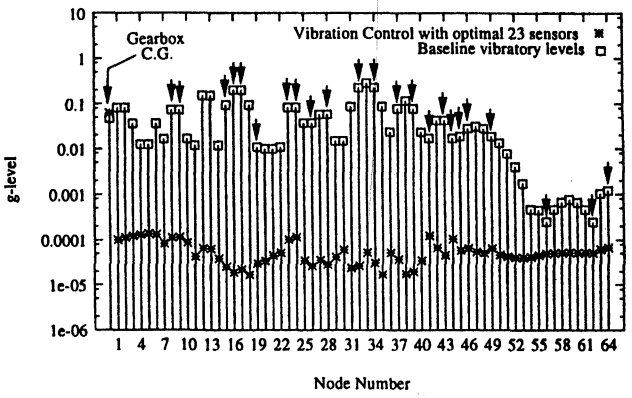

Fig. 8 Baseline vibration and controlled response (23 optimal sensors).

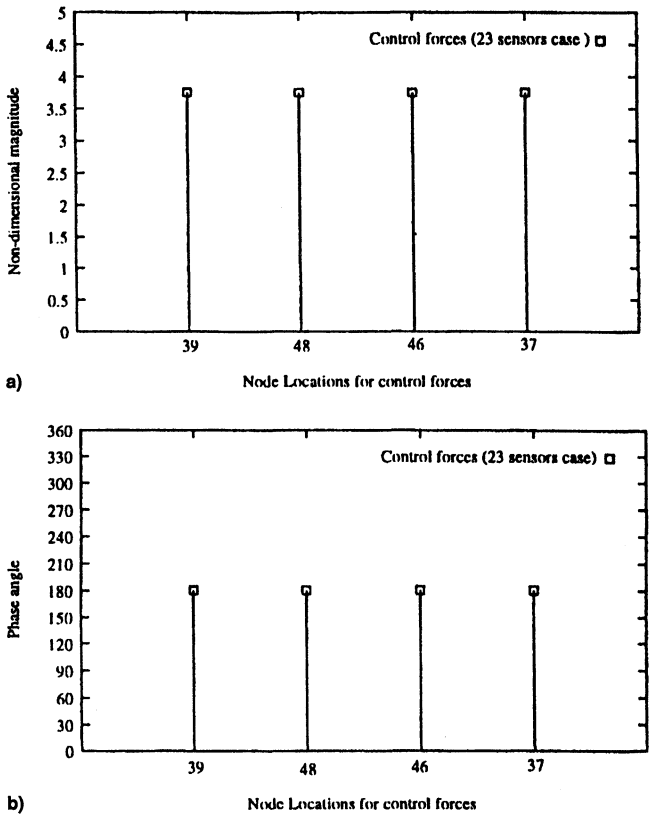

Fig. 9 a) Magnitude and b) phase angle of control forces.

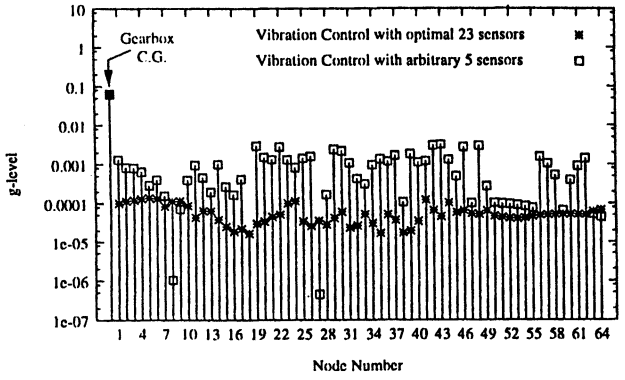

Fig. 10 Vibration control with 5 arbitrary sensors vs. control with 23 optimal sensors.

phase angles, respectively, of the four control forces required for vibration minimization. The control forces are almost 180 deg out-of-phase with the applied external force.

To analyze the effectiveness of vibration reduction using 23 optimally placed sensors, a vibration-reduction analysis using different sets of sensors located at arbitrary nodes in the fuselage was performed. The controlled response for these cases of arbitrary sensor locations was compared with the controlled response for the case of 23 optimally placed sensors. These results are shown in Figs. 10–13.

Figure 10 shows the results of the controlled vibratory response obtained using 5 arbitrary sensors and 23 optimally placed sensors. It is observed that the peak acceleration of the controlled response with five arbitrary sensors is 0.31E-02g at node location 43. The peak acceleration of the controlled response for 23 optimally placed sensors is 0.138E-03g at node location 5. Figure 11 shows a comparison of the controlled vibration with 10 arbitrary sensors and 23 optimally placed sensors. For the case of 10 arbitrary sensors, the peak acceleration of the controlled response is 0.211E-03g at node location 33, which is about 53% more than that for the case of 23 optimally placed sensors. Figure 12 shows the controlled response for the case of 23 arbitrary (nonoptimal set) sensors along with the controlled response with 23 optimally placed sensors. For the case of 23 arbitrary sensors, the peak acceleration is found to be 0.203E-03g at node location 41, which is 47% more than that for the case of 23 optimally placed sensors. The magnitudes and phase angles of the control forces for all of these case are presented in Table 2. It is interesting to note that though there is very small variation in the magnitudes and phase angles of the control forces, there seems to be a large variation in the peak acceleration of the controlled vibratory response of the fuselage. These results clearly indicate that vibration control using measurements from optimally

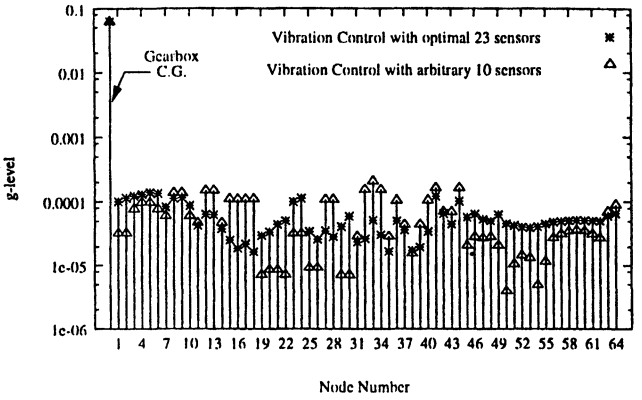

Fig. 11 Vibration control with 10 arbitrary sensors vs. control with 23 optimal sensors.

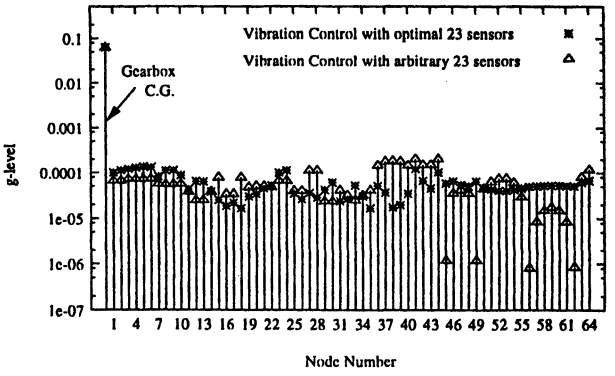

Fig. 12 Vibration control with 23 arbitrary sensors vs. control with 23 optimal sensors.

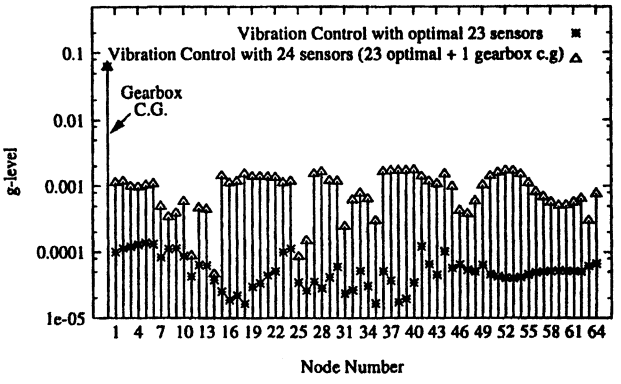

Fig. 13 Vibration control with 24 sensors vs. control with 23 optimal sensors.

Table 2 Magnitude and phase angle of control forces

Control force		Number of sensors used for vibration control				
Force	Node location	5 arbitrary	10 arbitrary	23 optimal	23 arbitrary (nonoptimal)	24 23 optimal + 1 gearbox
Magnitude	39	3.756	3.755	3.755	3.755	3.989
	48	3.756	3.756	3.755	3.756	3.561
	46	3.757	3.756	3.755	3.756	3.563
	37	3.756	3.755	3.755	3.755	3.978
Phase angle, deg	39	180.2	180.5	180.4	180.6	180.5
	48	182.4	180.3	180.4	180.3	180.2
	46	178.8	180.3	180.4	180.3	180.2
	37	180.5	180.5	180.4	180.6	180.5

placed sensors provide the minimum peak acceleration in the fuselage.

It is observed that even though there is vibration reduction in the fuselage, the gearbox c.g. experiences an increase in the acceleration level (Figs. 10–12). Therefore, an attempt was made to reduce simultaneously the vibratory levels at the gearbox c.g. as well as at the fuselage. In this case, the control forces required for vibration minimization were obtained using measurements from 24 sensors (23 optimal sensor locations in the fuselage + 1 sensor at the gearbox c.g.). Figure 13 shows the comparison of controlled vibratory levels obtained by using measurements from 23 optimal locations and those for the case of 24 sensors. It is interesting to observe that with 24 sensors there is no improvement in vibratory levels at the gearbox c.g., but there is deterioration in the control of fuselage vibratory levels. The magnitudes and phase of the control forces are given in Table 2. These values indicate that the vibratory levels are very sensitive to the control forces.

IV. Concluding Remarks

The problem of vibration reduction in helicopter fuselage, using the concept of ACSR, has been formulated. The equations of motion representing the dynamics of a coupled gearbox–fuselage model have been derived. Using these equations, the following studies have been performed. They are 1) identification of optimal sensor locations for vibration measurement and 2) formulation and solution of MIMO control scheme for vibration minimization in a helicopter fuselage. The salient points of this study are summarized next.

1) A detailed description of the EIDV approach for the identification of sensor locations for vibration measurement is presented.

2) Irrespective of the input excitation frequency, the optimal sensor locations identified by the single elimination process experience high levels of vibration.

3) Vibration control using measurements from the optimally selected sensor locations provides maximum reduction in the g levels of the fuselage vibration as compared with the controlled response using measurements from arbitrarily placed sensor locations or from a nonoptimal set of sensors.

4) When the vibratory levels in the fuselage are minimized, the gearbox experiences a higher level of vibration in comparison with the baseline g level. While trying to minimize simultaneously the vibratory levels in the fuselage and gearbox, it was observed that there is no reduction in the vibratory levels at the gearbox, but the reduction in fuselage vibratory levels is not as significant as in the optimal case.

Acknowledgments

The financial support from the Structures Panel of the Aeronautics Research and Development Board is gratefully acknowledged. The authors thank the reviewers for their critical comments.

References

[1]Reichert, G., "Helicopter Vibration Control—A Survey," *Vertica*, Vol. 5, No. 1, 1981, pp. 1–20.

[2]Loewy, R. G., "Helicopter Vibrations: A Technological Perspective," *Journal of the American Helicopter Society*, Vol. 29, No. 4, 1984, pp. 4–30.

[3]Kvaternik, R. G., Bartlett, F. D., Jr., and Cline, J. H., "A Summary of Recent NASA/ARMY Contributions to Rotorcraft Vibrations and Structural Dynamics Technology," *NASA/ARMY Rotorcraft Technology*, NASA CP-2495, 1988, pp. 71–179.

[4]Crews, S. T., "Rotorcraft Vibration Criteria: A New Perspective," *Proceedings of the 43rd Annual Forum of the American Helicopter Society* (St. Louis, MO), American Helicopter Society, Alexandria, VA, 1987, pp. 991–998.

[5]King, S. P., and Staple, A. E., "Minimization of Vibration Through Active Control of Structural Response," *Rotorcraft Design Operations*, AGARD, CP-423, 1986, pp. 14.1–14.13.

[6]Staple, A. E., "An Evaluation of Active Control of Structural Response as a Means of Reducing Helicopter Vibration," *Proceedings of the 15th European Rotorcraft Forum* (Amsterdam, The Netherlands), 1989, pp. 3–17.

[7]Welsh, W. A., Von Hardenberg, P. C., Von Hardenberg, P. W., and Staple, A. E., "Test and Evaluation of Fuselage Vibration Using Active Control of Structural Responses (ACSR) Optimized to ADS-27," *Proceedings of the 46th Annual Forum of the American Helicopter Society* (Washington, DC), American Helicoptor Society, Alexandria, VA, 1990, pp. 21–37.

[8]Reichert, G., and Huber, H., "Active Control of Helicopter Vibration," *Proceedings of the 4th Workshop on Dynamics and Aeroelastic Stability Modelling of Rotorcraft Systems*, Univ. of Maryland, College Park, MD, 1991, pp. 1–20.

[9]Welsh, W., Fredrickson, C., Rauch, C., and Lyndon, I., "Flight Test of an Active Vibration Control System on the UH-60 Black Hawk Helicopter," *Proceedings of the 51st Annual Forum of the American Helicopter Society* (Fort Worth, TX), American Helicoptor Society, Alexandria, VA, 1995, pp. 393–402.

[10]Chiu, T., and Friedmann, P. P., "ACSR System of Vibration Suppression in Coupled Helicopter Rotor/Flexible Fuselage Model," *Proceedings of the AIAA/ASME/ASCE/AHS/ASC 37th Structures, Structural Dynamics, and Materials Conference* (Salt Lake City, UT), AIAA, Reston, VA, 1996, pp. 1972–1990.

[11]Kammer, D. C., "Sensor Placement for On-Orbit Modal Identification and Correlation of Large Space Structures," *Journal of Guidance, Control, and Dynamics*, Vol. 14, No. 2, 1991, pp. 251–259.

[12]Lim, T. W., "Actuator/Sensor Placement for Modal Parameter Identification of Flexible Structures," *Modal Analysis: The International Journal of Analytical and Experimental Modal Analysis*, Vol. 8, No. 1, 1993, pp. 1–13.

[13]Penny, J. E. T., Friswell, M. I., and Garvey, S. D., "Automatic Choice of Measurement Locations for Dynamic Testing," *AIAA Journal*, Vol. 32, No. 2, 1994, pp. 407–414.

[14]Kubrusly, C. S., and Malebranche, H., "Sensors and Controllers Location in Distributed Systems—A Survey," *Automatica*, Vol. 21, No. 2, 1985, pp. 117–128.

[15]Stoppel, J., and Degener, M., "Investigations of Helicopter Structural Dynamics and a Comparison with Ground Vibration Tests," *Journal of the American Helicopter Society*, Vol. 27, No. 2, 1982, pp. 34–42.

[16]Udayasankar, A., "Choice of Sensor Locations and Vibration Control in Flexible Fuselage System," M. Tech. Thesis, Dept. of Aero-

space Engineering, Indian Inst. of Technology, Kanpur, India, 1997.

[17]Garybill, F. A., *Matrices with Application in Statistics*, 2nd ed., The Wardsworth Statistical/Probability Series, Wardsworth, Inc., Belmont, CA, 1983, pp. 108–136, 418–430.

[18]Leon, S. J., *Linear Algebra with Applications*, 2nd ed., Macmillan, New York, 1986, pp. 321–325.

[19]Venkatesan, C., and Udayasankar, A., "Choice of Measurement Locations for Active Vibration Control in Helicopters," *Proceedings of the CEAS International Forum on Aeroelasticity and Structural Dynamics* (Rome), Vol. 2, 1997, pp. 335–342.

[20]Mangalick, S., Venkatesan, C., and Kishore, N. N., "Formulation and Dynamic Analysis of a Helicopter Fuselage Model," TR IITK/AE/ARDB/AVCH/826/95/01, Dept. of Aerospace Engineering, Indian Inst. of Technology, Kanpur, India, 1995.

[21]Sivaramakrishnan, R., Venkatesan, C., and Varadan, T. K., "Rotor/Fuselage Vibration Isolation Studies by a Floquet-Harmonic Iteration Technique," *Journal of Aircraft*, Vol. 27, No. 1, 1990, pp. 81–89.